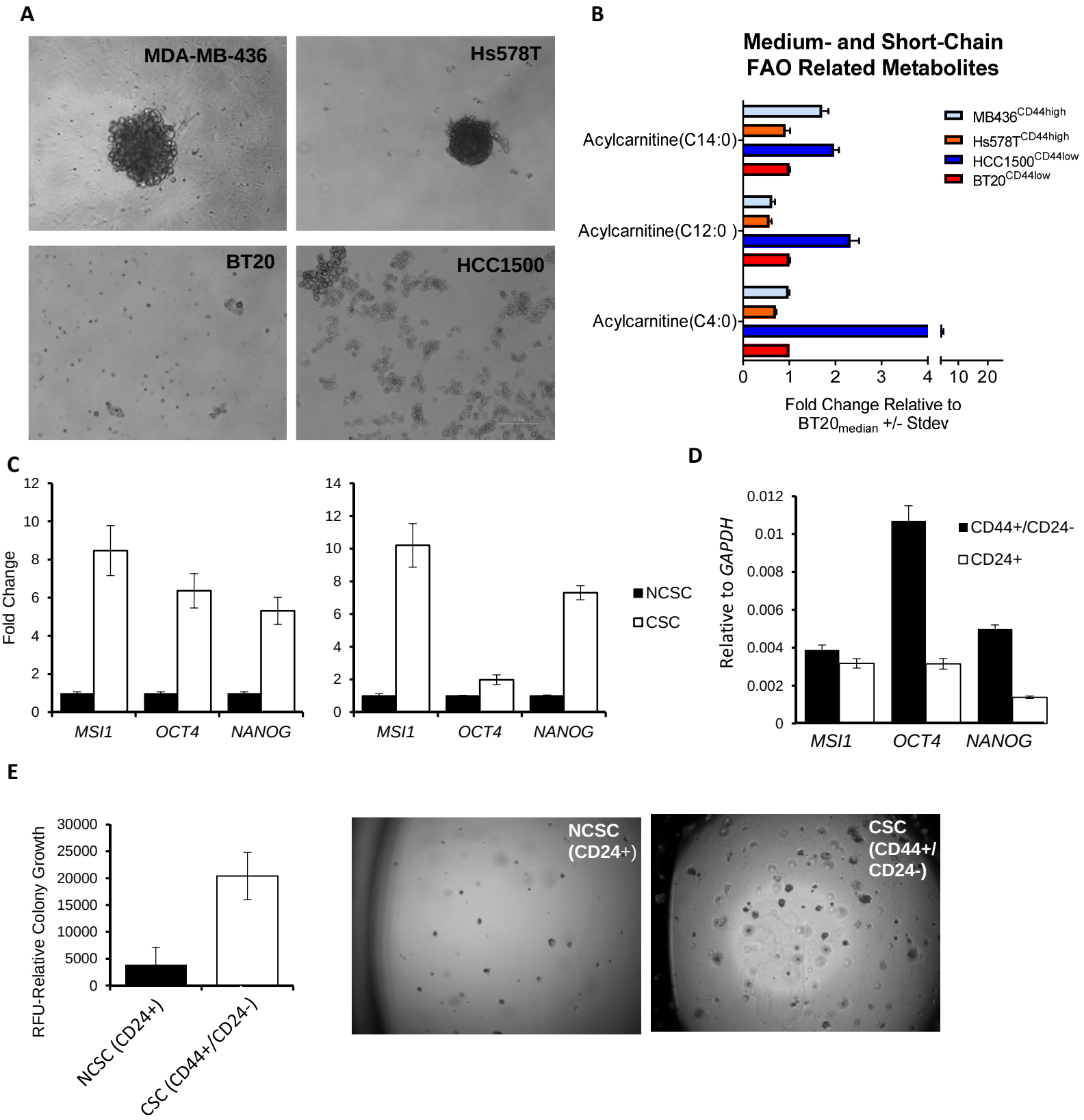

Supplemental Figure 1.Related to Figure 1 and 2. (A) Tumorsphere formation results for CD44+/CD24- BCSC cell lines MDA-MB-436 (top left) and Hs578T (top right) and CD24+ NCSC cell lines BT20 (bottom left) and HCC1500 (bottom right). (B) Fold-change in medium- and short-chain fatty acylcarnitines in Hs578T, MDA-MB-436 and HCC1500 relative to BT20. C to E, BBM2 and BBM3 Tumorspheres and CD44+/CD24- MDA-MB-468 exhibit stem-like properties. (C) Real time PCR comparing gene expression of *MSI1*, *OCT4*, and *NANOG* in BBM2 and BBM3 tumorspheres with their adherent counterparts. Values are represented as fold change to adherent cells. Shown are mean ± SD (*n*=3). (D) Real time PCR comparing mRNA levels of *MSI1*, *OCT4*, and *NANOG* in CD44+/CD24- and CD24+ MDA-MB-468 cells. Shown are mean ± SD (*n*=3). (E) Soft agar colony assay comparing colony-forming ability of CD44+/CD24- and CD24+ MDA-MB-468 cells. Right, phase contrasts images of colonies. Shown are mean ± SD (*n*=4).

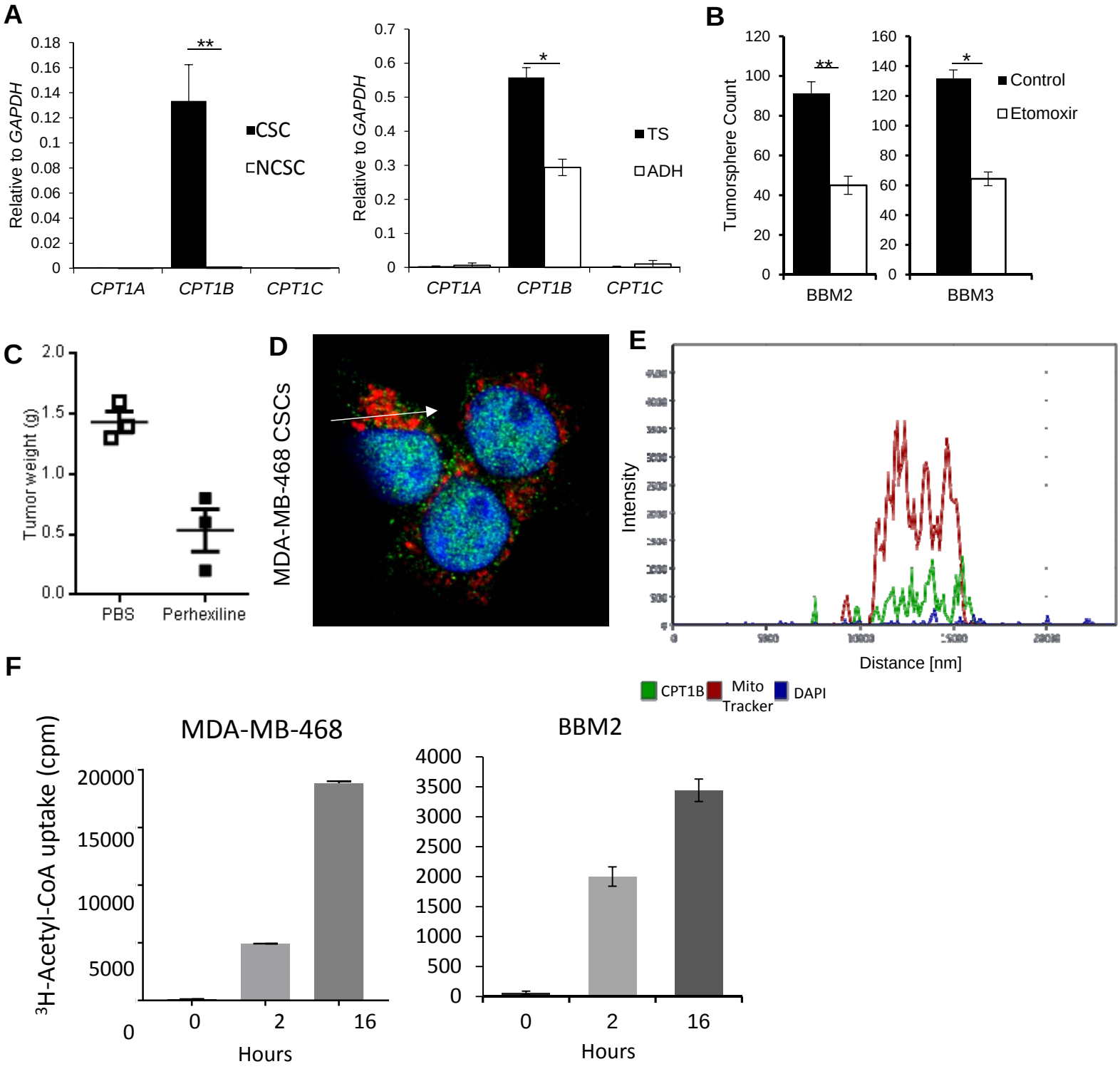

Supplemental Figure 2. **BCSCs Highly Express CPT1B.** Related to Figure 3 to 4. (A) Real-time PCR measuring mRNA expression levels of CPT1 isoforms in CSC (CD44+/CD24-) versus NCSC (CD24+) MDA-MB-468 cells (left panel), and in BBM2 tumorspheres (TS) versus adherent cells (ADH) (right panel). Shown are mean ± SD (*n*=3). (B) Tumorsphere formation of BBM2 and BBM3 tumorspheres treated with 50 µM etomoxir for 16 hours. Tumorsphere count was then normalized with control treatment. (C) Tumor weight of *MMTV-PyMT* mice treated with 5 mg/kg perhexiline every two days for three weeks before harvested. D and E, colocalization analysis of CPT1b with mitochondria. (D) CD44+/CD24- MDA-MB-468 cells were stained with 200 nM MitoTracker (red) and CPT1B (green). (E) The diagram shows the colocalization analysis using fluorescence-intensity profiles of both fluorescent signals. (F) Acetyl-Coenzyme A uptake assay. CSCs from MDA-MB-468 and tumorspheres from BBM2 were cultured with 1 µM of Acetyl-coA and 5 µCi of ^{3}H-Acetyl-CoA mixture at the indicated times. After three washes with PBS, the cells were harvested and lyzed. ^{3}H-Acetyl-CoA uptake was measured by liquid scintillation counting.

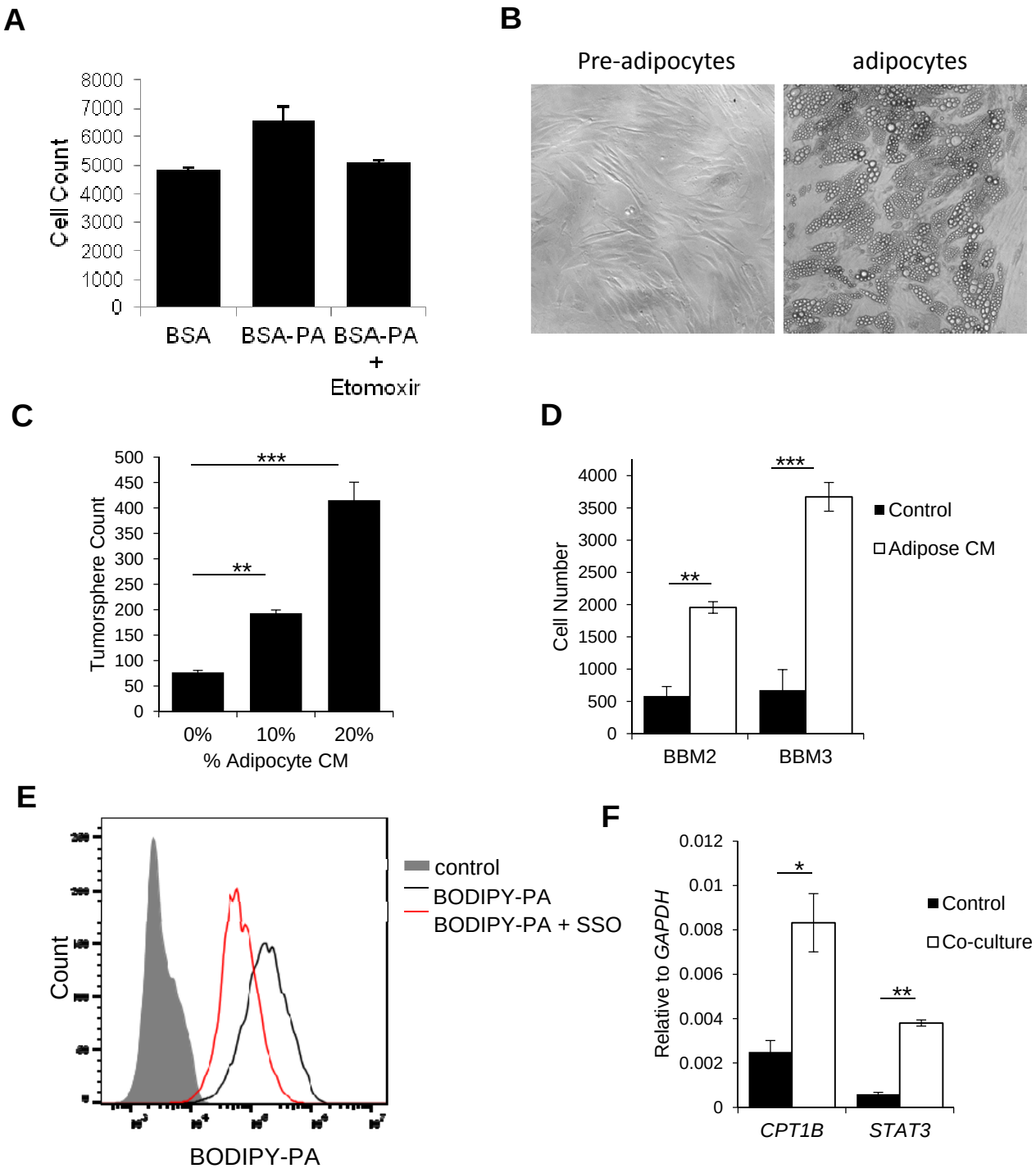

Supplemental Figure 3. BCSCs Utilize Adipocyte-Derived Lipids to Drive Self-Renewal. Related to Figure 5. (A) BBM2 tumorspheres count after treatment with BSA or BSA-PA. Shown are mean ± SD (*n*=3). (B) left panel, phase contrast microscopy of human breast pre-adipocytes day 0 of differentiation; right panel, phase contrast microscopy of human breast adipocytes at day 14 after differentiation. (C) BBM2 tumorsphere formation in culture after supplemented with increasing concentrations of human breast adipocyte conditioned medium. Shown are mean ± SD (*n*=3). (D) Cell migration assay of BBM2 and BBM3 tumorsphere migrating toward human breast adipocyte conditioned media. Shown are mean ± SD (*n*=3). (E) Lipid uptake assay demonstrating fluorescent palmitic acid uptake of BBM2 cells from breast adipocyte (black line). SSO was added to adipocyte and BBM2 co-culture to block fluorescent palmitic acid uptake (red line).Shown is average of three independent experiments. (F) Real-time PCR of *CPT1B* and *STAT3* mRNA transcripts in BBM2 tumorspheres after co-culturing with human breast adipocytes. Shown are mean ± SD (*n*=3).

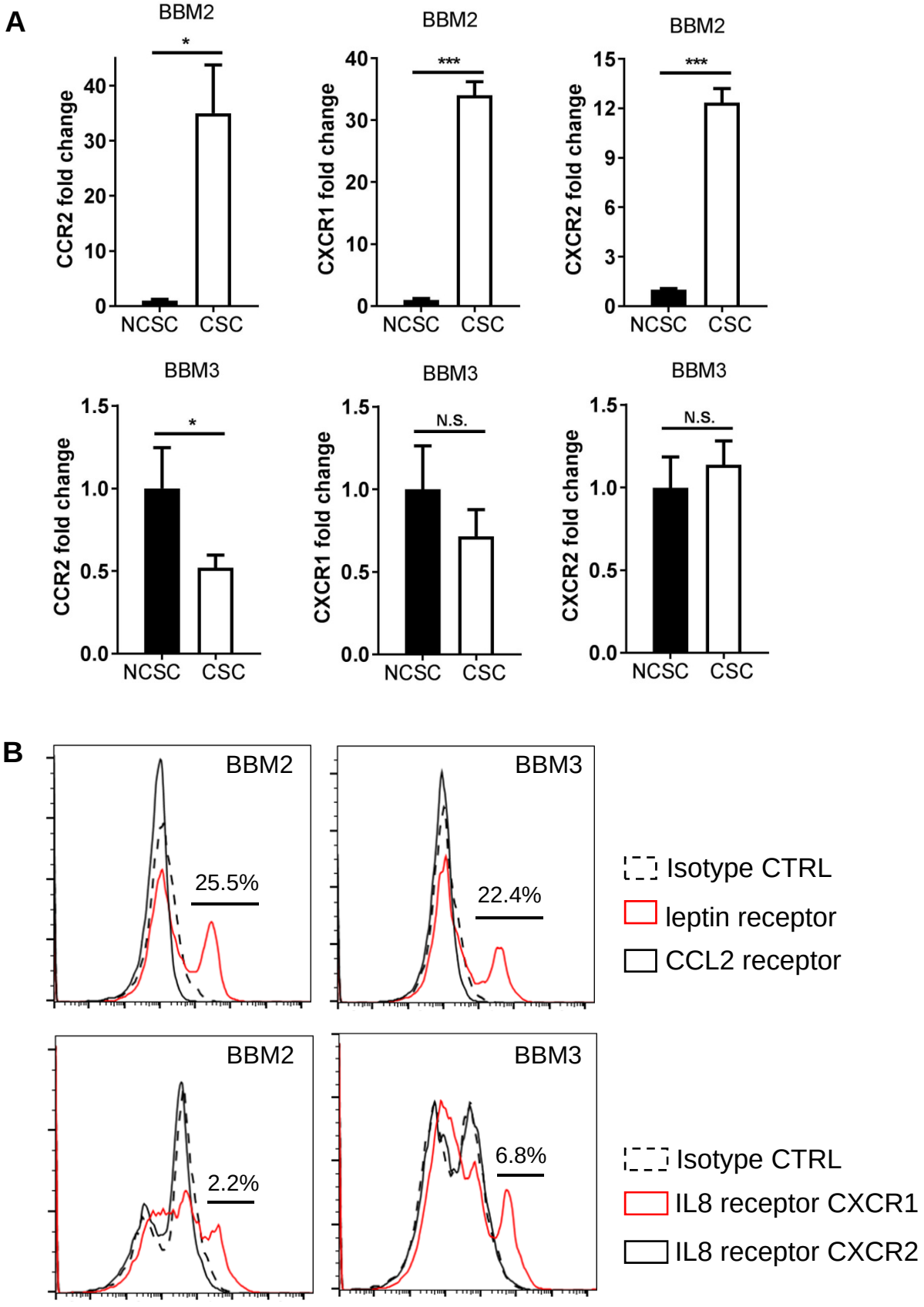

Supplemental Figure 4. BCSCs Highly Express Leptin Receptor. Related to Figure 5. (A) Real-time PCR showing the mRNA expression levels of CCL2 receptor (CCR2), and IL-8 receptors (CXCR1, and CXCR2). Shown are mean ± SD (n=3). * $p < 0.01$, ** $p < 0.001$, *** $p < 0.0001$. (B) Flow cytometric analysis of leptin receptor and 3 other receptors for adipokines, including CCL2 receptor and IL-8 receptors.

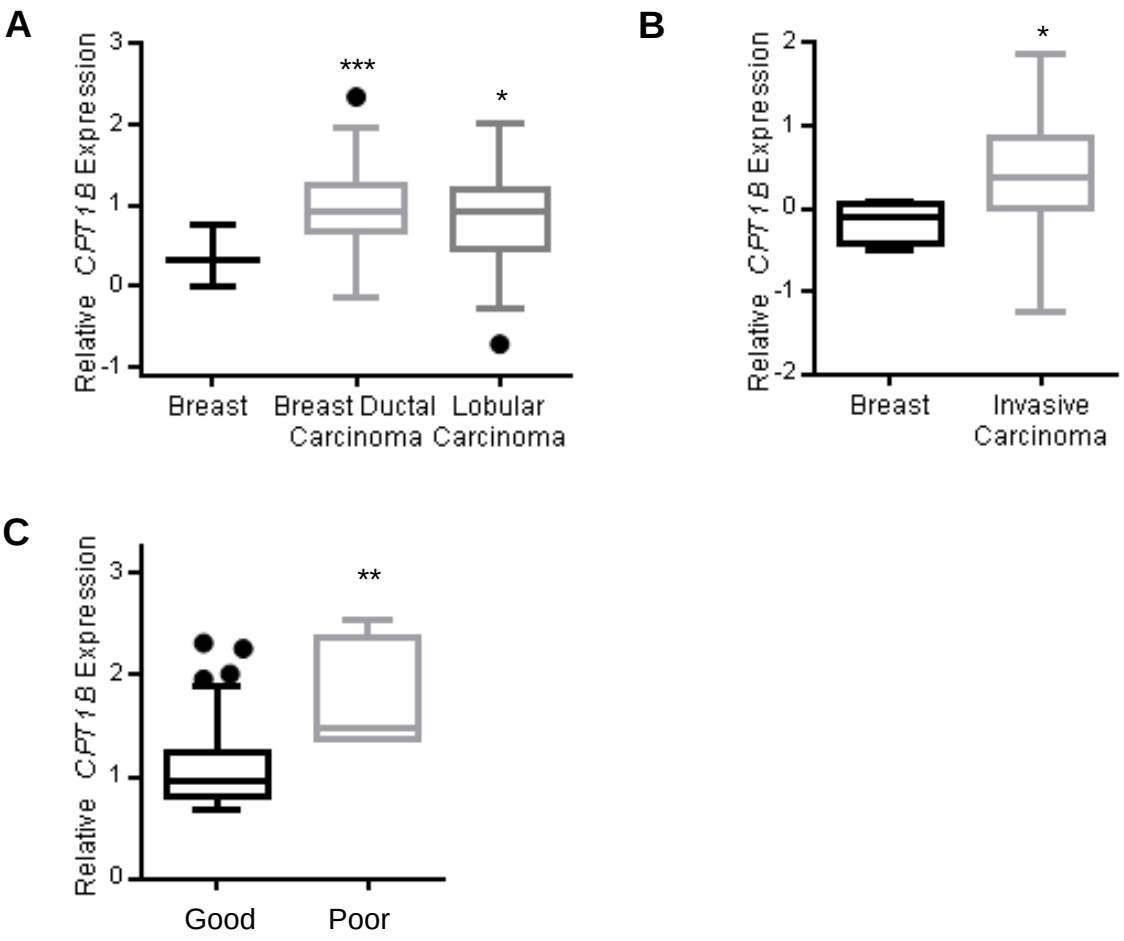

Supplemental Figure 5. **CPT1B is Significantly Increased in Breast Carcinomas and Correlates with Poor Clinical Outcome.** Related to Figure 6. (A) Oncomine analysis of Zhao breast cancer database comparing *CPT1B* mRNA expression in normal breast tissue (*n*=3) vs. breast ductal carcinoma (*n*=37) and lobular carcinoma (*n*=20). (B) Oncomine analysis of Gluck breast cancer database comparing *CPT1B* mRNA expression in normal breast tissue (*n*=4) vs. invasive breast carcinoma (*n*=154). (C) Oncomine analysis of Finak breast cancer database comparing *CPT1B* expression in patients with good (*n*=43) vs. poor outcome (*n*=6).

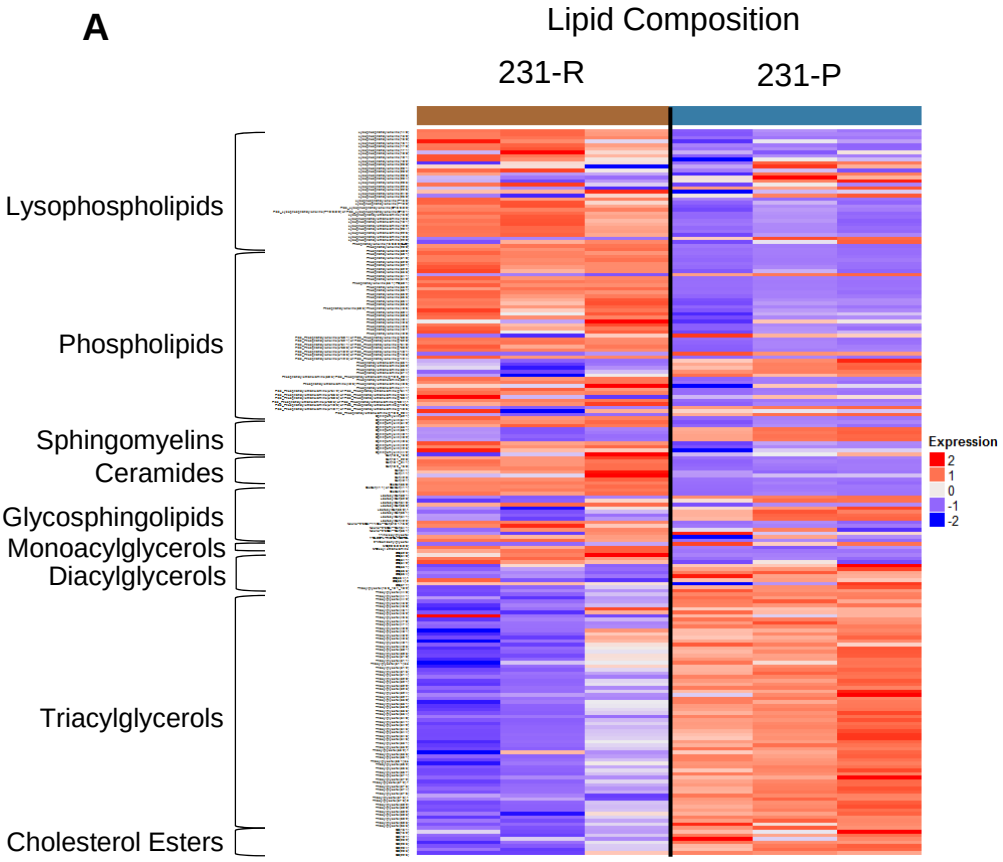

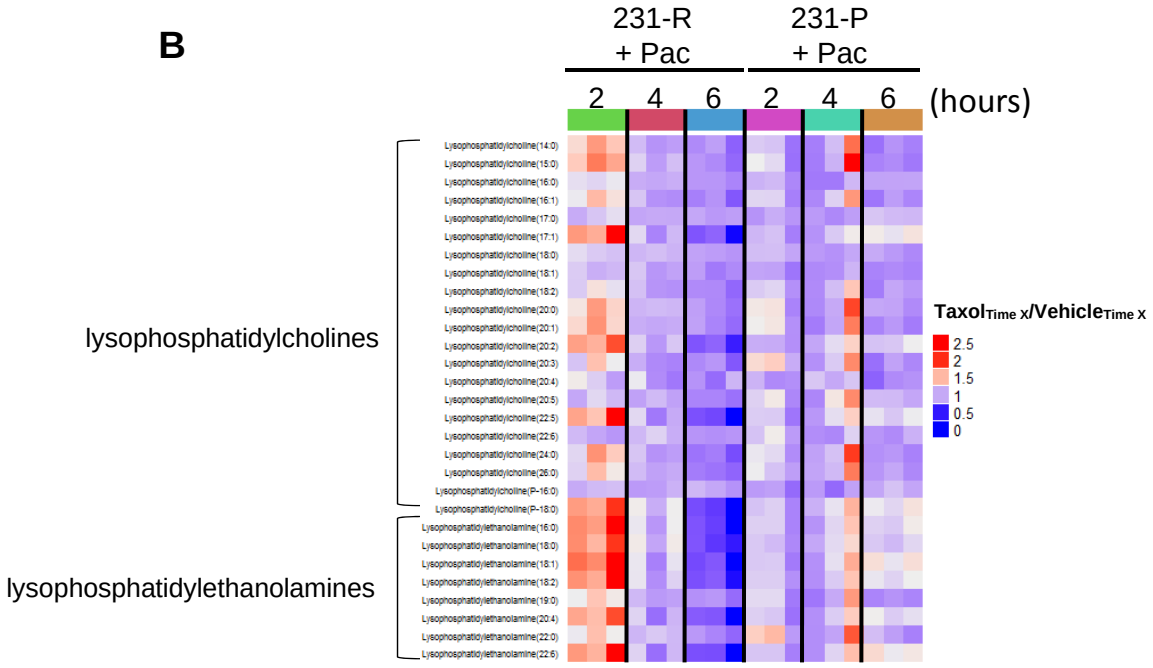

Supplemental Figure 6. Related to Figure 7. (A) Heatmap depicting levels of detected lipids in MDA-MB-231 chemoresistant (231-R) and parental (231-P) TNBC cell lines. Values were autoscaled. Brackets on the left designate the lipid domains associated with the respective individually detected lipids. (B) Heatmap illustrating fold-change in respective lysophospholipids following 2, 4 or 6 hours of paclitaxel challenge in chemoresistant MDA-MB-231 (231-R) and parental (231-P) TNBC cell lines relative to respective time-matched vehicle (DMSO) controls. Brackets distinguish lysophosphatidylcholines (top) from lysophosphatidylethanolamines (bottom).

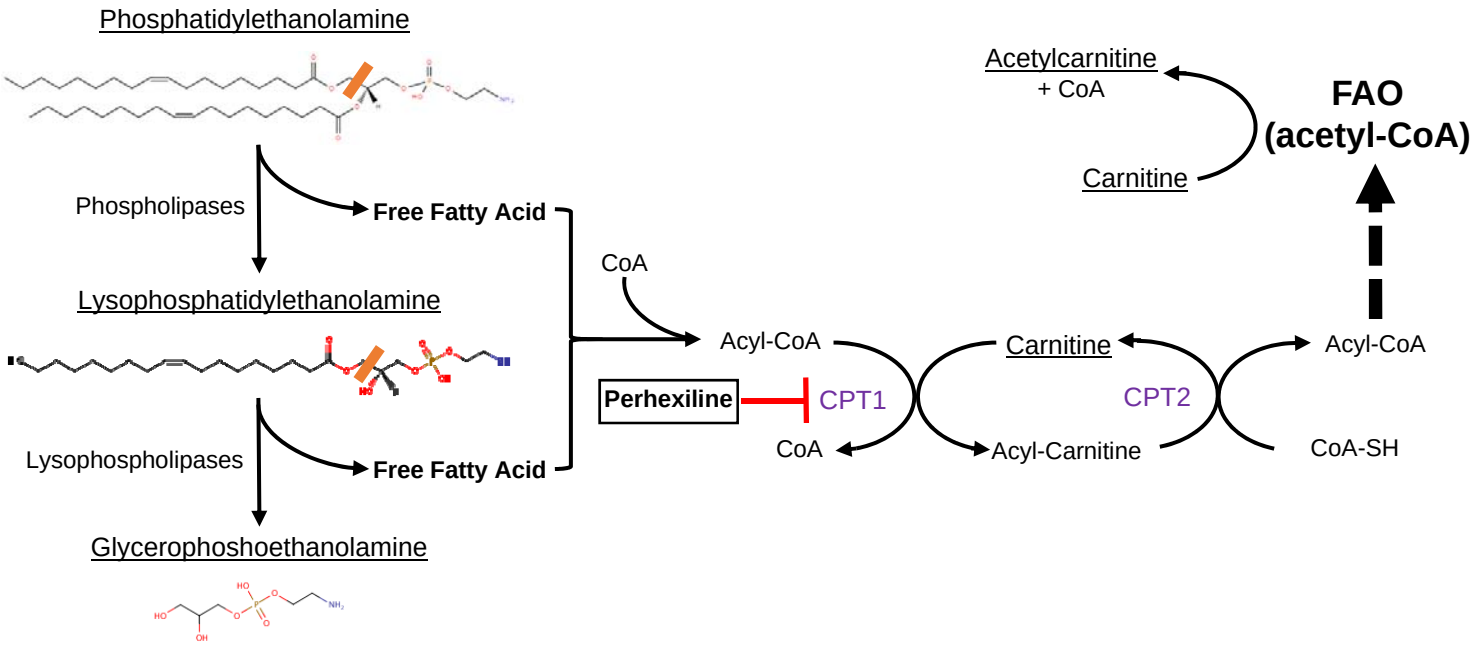

Supplemental Figure 7. **Proposed interpretation of metabolomic results for 231-R cells following paclitaxel challenge.** Related to Figure 6 and 7. Following addition of paclitaxel, 231-R TNBC cells exhibit sequential lipolysis of phosphatidylethanolamines resulting in two free fatty acids and the glycerophosphoethanolamine head group as cleavage products. Free fatty acids are subsequently available for FAO via the carnitine-shuttle pathway. Inhibition of CPT1 via perhexiline inhibits the transfer of LCFA into the mitochondrial matrix for FAO.

Supplemental Table 1 – Related to STAR Methods, including CPT1B Promoter Reporter Assay, Chromatin Immunoprecipitation Assay and Real-Time PCR throughout the study. Primer sequence and source

GENE NAME	SOURCE	IDENTIFIER
CPT1B promoter F- ATCGCTTGAGCTCCGGGCAGAAGTGCCAGCCAAGG	This paper	N/A
CPT1B promoter R- ATCGCTTCTCGAGAGAGGAAAGAGGGATTGGGGAAGAGGC	This paper	N/A
hActin-F-CATCGAGCACGGCATCGTCA	This paper	N/A
hActin-R- TAGCACAGCCTGGATAGCAAC	This paper	N/A
hCCR2-F- CTGAGACAAGCCACAAGCTG	This paper	N/A
hCCR2-R- TCACCGCTCTCGTTGGTATT	This paper	N/A
hCXCR1-F- TACTGTTGGACACACCTGGC	This paper	N/A
hCXCR1-R- GGCATGCCAGTGAAATTTAG	This paper	N/A
hCXCR2-F- AGCAGGTCACAGCTGCTCTT	This paper	N/A
hCXCR2-R- TCTTCAAAGCTGTCACTCTCCA	This paper	N/A
hLEPR-F- CTTATGCTGGGATGTGCCTT	This paper	N/A
hLEPR-R- CCCAATGTAACAAAACCACACA	This paper	N/A
CPT1B-F	RealTimePrimer.com	Cat# VHPS-2185
CPT1B-R	RealTimePrimer.com	Cat# VHPS-2185
CPT1A-F	RealTimePrimer.com	Cat# VHPS-2184
CPT1A-R	RealTimePrimer.com	Cat# VHPS-2184
CPT1C-F	RealTimePrimer.com	Cat# VHPS-2186
CPT1C-R	RealTimePrimer.com	Cat# VHPS-2186
ACADM-F	RealTimePrimer.com	Cat# VHPS-73
ACADM-R	RealTimePrimer.com	Cat# VHPS-73
MSI1-F	RealTimePrimer.com	Cat# VHPS-5899
MSI1-R	RealTimePrimer.com	Cat# VHPS-5899
OCT4(POU5F1)-F	RealTimePrimer.com	Cat# VHPS-7107
OCT4(POU5F1)-R	RealTimePrimer.com	Cat# VHPS-7107
STAT3-F	Qiagen	Cat# PPH00708F-200
STAT3-R	Qiagen	Cat# PPH00708F-200
NANOG-F	RealTimePrimer.com	Cat# # VHPS-6043
NANOG-R	RealTimePrimer.com	Cat# # VHPS-6043